Multiscale Extraction and Representation of Features from Medical Images

Marta Fidrich, Jean-Philippe Thirion

INRIA

INSTITUT NATIONAL DE RECHERCHE EN INFORMATIQUE ET EN AUTOMATIQUE

Multiscale Extraction and Representation of Features from Medical Images

Márta Fidrich , Jean-Philippe Thirion

N° 2365

Octobre 1994

PROGRAMME 4

Robotique,

image

et vision

1994

ISSN 0249-6399

INRIA
SOPHIA ANTIPOLIS

Multiscale Extraction and Representation of Features from Medical Images

Márta Fidrich *, Jean-Philippe Thirion **

Programme 4 — Robotique, image et vision
Projet Epidaure ***

Rapport de recherche n° 2365 — Octobre 1994 — 28 pages

Abstract:

For automatic registration of medical images, we must search for geometric features that are invariant both with respect to rigid transformations and to smooth changes of resolution. Beginning with Witkin's seminal paper, scale space theory provides an elegant framework for studying the multiscale behavior of these characteristics. However, a natural scale-space representation of features, useful for practical applications, is still missing.

We address here the problem of multiscale extraction and representation of characteristic points based on iso-surface techniques. Our main concern is with $2D$ images: we analyze corner points at increasing scales using the Marching Lines algorithm. Since we can exploit the intrinsic nature of intensity of medical images, segmentation of components or parameterization of curves is not needed, in contrast with other methods. Due to the direct use of the coordinates of points, we get a representation of orbits, which is very convenient both for detection at coarse scale and for localization at fine scale. We find that the significance of corner points depends not only on their scale-space lifetime but also on their relationship with curvature inflexion points.

Key-words: Scale space, Differential geometry, Singularity theory

(Résumé : tsvp)

*e-mail: marta.fidrich@sophia.inria.fr
**e-mail: jean-philippe.thirion@sophia.inria.fr
***http://zenon.inria.fr:8003/Equipes/EPIDAURE-eng.html

Unité de recherche INRIA Sophia-Antipolis
2004 route des Lucioles, BP 93, 06902 SOPHIA-ANTIPOLIS Cedex (France)
Téléphone : (33) 93 65 77 77 – Télécopie : (33) 93 65 77 65

Extraction et representation multi-échelle des caractéristiques d'images médicales

Résumé :

Pour le recalage automatique d'images médicales, il faut chercher des caractéristiques géométriques invariantes à la fois par toute transformation rigide et par tout changement léger de la résolution. Depuis l'article fondamental de Witkin, la théorie de l'espace multi-échelle fournit un outil de travail élégant pour étudier le comportement de ces caractéristiques. Cependant, il manque toujours une représentation naturelle de caractéristiques dans l'espace multi-échelle, utile pour des applications pratiques.

Nous nous intéressons dans ce papier au problème de l'extraction et de la représentation de points caractéristiques, toutes deux basées sur des techniques d'iso-surfaces. Nos travaux portent sur les images bidimensionnelles : nous analysons des points de coin à des échelles grandissantes, en utilisant l'algorithme des Marching Lines. En exploitant la nature intrinsèque de l'intensité dans les images médicales, nous nous affranchissons de toute segmentation d'éléments ou d'une quelconque paramétrisation des courbes, à la différence des autres méthodes. Grâce à l'utilisation directe des coordonnées des points, nous obtenons une représentation d'orbites qui est très pratique aussi bien pour la détection à des échelles grossières qu'à la localisation à des échelles plus fines. Nous trouvons que la signification des points de coin dépend non seulement de leur durée de vie mais aussi de leur lien avec des points d'inflexion.

Mots-clé : Espace multi-échelle, Géométrie différentielle, Théorie de la singularité

1 Introduction

In practice, the relevant details of images exist only within a restricted range of scales. We call the size of the smallest, still recognizable features in an image the inner scale, which is determined by the imaging device, while the extent, or the largest scale represented in an image is called the outer scale. In *shape description* we search for significant features (structures) between these limits. To measure the significance of structures, we have to compute some qualitative descriptions, where we also have the problem of scale, for example: a derivative must be taken in some neighborhood, but there is seldom a principled basis for choosing its size. These facts have led to the development of *scale space theory*, whose basic concept can be summarized as follows. If our aim is to retain all available structures, then we must treat the image at all levels of resolution simultaneously and we should understand the relation of derived images at different levels of scale (which presuppose the existence of links between them).

Beginning with Witkin's pioneering paper [21], there have seen many interesting works over the past decade. Research emphasizes two main topics:

- how to construct the best discretized multiscale representation
- how the individual features behave and how to apply this knowledge to various problems, e.g. matching and recognition

If we restrict ourselves to medical image processing, we can exploit its specific properties very fruitfully. For example, the geometric measurements are Euclidean, and not projective, contrary to video images of a $3D$ scene. Moreover, the value of intensity is intrinsic, because it is generally related in a simple way to the physical or physiological properties of the considered organs. This is why the use of iso-surface techniques is widespread among practical applications. In many cases the iso-surface can be extracted directly. Sometimes, however, a pre-segmentation step is required to determine which part of the image is the object and which part is the background. This pre-segmentation, composed with smoothing filters, morphological operators and search of connected components, leads to a $3D$ image, where the intensity roughly represents the probability of being inside or outside of the object. Iso-surface techniques are then used in the final phase to extract the object, or

rather some characteristics of it (among several works see e.g. Lorensen and Cline [11], Thirion and Gourdon [18] or Udupa [20]).

Organs are generally bounded with smooth surfaces, hence features defined by curvatures are particularly meaningful. For example, *corner points* characterized by the local extrema of the isophote curvature on a $2D$ slice, or *crest lines* in $3D$, which are the lines corresponding to the successive loci of the isosurface whose principal curvature is locally extremal are already established as significant features (see Thirion and Gourdon [17]).

Features which can be defined as zero-crossings of (possibly non-linear) differential expressions are called *differential singularities*. The singularity set of a differential operator changes with the scale parameter: the orbits of singularity points in the scale-extended space may undergo *bifurcations*, splitting or merging. The points of bifurcation on the orbits of differential singularities are called *catastrophe points*. The frequently used *critical points* mean a subset of differential singularities, which are defined by the zero-crossings of the gradient. The critical points are classified by their Hessian: they are minima, maxima or saddle points depending on whether the Hessian matrix is positive definite, negative definite or indefinite. Furthermore, they are called nongeneric if their Hessian matrix is singular; intuitively this means that they are unstable since small perturbations change their nature.

Theoretical results about the behavior of singularities have been obtained only in simple cases. Typically, the evolution of 2-3 isolated critical points have been analyzed in generality (see e.g. Gauch and Pizer [6], or Johansen [7]). Alternatively, a more general singularity, let us say a corner point, has been examined, but only in the case of simple (parameterized) contour models (see Asada and Brady [1]). In practice, the set of configurations can be huge, so it is too difficult to depict all the influences together of some chosen singularities. This is why we need to exemplify the orbits of some features in scale space, and to do so is the goal of this paper.

In section 2, we give a brief survey on the current research, both on the theory and on the applications. The next section deals with the problems of construction of discrete scale-space images. In section 4, we show a natural way to visualize multiscale properties. Finally, in section 5 we analyze the behavior of curvature inflexions and corner points in scale space.

2 Overview on scale space

2.1 Theoretical results

To obtain the multiscale extension of an image, we must convolve it with smoothing filters scaled by a parameter, let say $t \in I\!R_+$, as Koenderink has formulated [8]:

- Embed the original image $f(\mathbf{r})$ into a family of smoothed images $\varphi(\mathbf{r}, t)$ so that $\varphi(\mathbf{r}, 0) = f(\mathbf{r})$.
  The parameter t measures resolution, or inner scale, while the outer scale determines how far to proceed.
- Study the family, that is, the relations between structural features. (deep structure investigation)
- If it is possible, build a model which uses the relations discovered. (applications to matching, recognition)

A number of papers have been published exploring the theory of scale space. For example, Babaud [2], Yuille and Poggio [22] and also Koenderink [8] have proved that the *Gaussian*

$$g(\mathbf{r}, \sigma) = \frac{1}{(2\pi)^{n/2}\sigma^n} \cdot e^{-\frac{\mathbf{r}^2}{2\sigma^2}} \quad \text{where} \quad \mathbf{r} = (x_1, \cdots, x_n)$$

is the only filter that leads to monotonous destruction of detail under consecutive blurring. More precisely, it satisfies the following nice scale behavior (among other interesting properties):

- as the scale σ increases no spurious detail is generated
- as the scale σ decreases no extremality (zero-crossings) vanishes

Consequently, each extremum can be characterized by the coarsest scale at which it appears and by its location at the finest scale of observation (thus correcting the distorting effects of smoothing).

There are different interpretations of the expression: "*no spurious detail is generated*" in one and higher dimensions. In the one dimensional case all the extrema become monotonically more pronounced and zero-crossing contours cannot in general vanish as the variance σ of the filter is decreased [2, 22]. In higher dimensions however, an extremum and a saddle point might be created

as the image is blurred, and also the zero-crossing contours, while they may not vanish, are free to split and merge; though any feature indeed possesses a "cause" at a finer level of resolution [22, 23]. The change of singularity set as well as the bifurcation events are more complicated in higher dimensions, for a detailed description see e.g. Lindeberg 's [10] or Johansen 's [7] work.

There are also some papers about how to compute practical representations of scale-space images. For instance, Lindeberg and Eklundh [9, 5] argue that the *discrete aspects of implementation* should be considered already in the theoretical formulation of the scale-space representation. Solving the discretized version of the diffusion equation, they have obtained the kernel (which approaches rapidly the Gaussian as it is scaled) $T : \mathbb{Z}^2 \times \mathbb{R}_+ \rightarrow \mathbb{R}$, defined by:

$$T(m, n, t) = e^{-2t} I_m(t) I_n(t)$$

where $I_m(t)$ and $I_n(t)$ are the modified Bessel functions of integer order. Unfortunately, there are no closed forms for the modified Bessel functions, nor for their derivatives, which makes difficult and time-consuming the numerical implementation.

Romeny, Florack et al [15, 14] emphasize the proper way of *differentiation* using the derivatives of the Gaussian as a class of scaled differential operators. They have also called the attention to the analogue of the human visual perception (the receptive fields) and of the scaled tensors.

2.2 Applications

Generally, the original image is first transformed into a multiscale representation, then this representation is processed, for example, to solve matching problems, or to search for stable significant characteristics.

Witkin's binary scale-space image and *interval-tree* [21] was the first multiscale representation for $1D$ signals. The function $f(x)$ is convolved with a Gaussian as its variance σ increases, and the zero-crossings of the second derivatives of each convolved function are extracted and marked in the $x - \sigma$ plane giving the scale-space image. This image is then collapsed into a discrete structure, the interval-tree, using the connectivity of extremal points tracked through scale, and also the catastrophe points at which new extrema appear.

He has also introduced the *hypothesis of stability* based on empirical observations: the extremal points that survive over a broad range of scale are more significant, more stable.

Yuille and Poggio [22] have proved a challenging result: the zero-crossings in scale space of almost all signals filtered by a Gaussian determine the signal uniquely up to a scaling constant. Further, Rotem and Zeevi [16] have shown under what conditions and *how 2D signals can be recovered* from their zero-crossings. This has an important consequence — for almost all signals — that no information is lost by working with the scale-space image, e.g. the matching can be solved reliably in scale space.

Mokhtarian and Mackworth [12] have extended Witkin's scale-space image to describe parameterized planar curves as *curvature scale-space image*s. It is produced by the convolution of the arc-length s parametric form of a curve with σ-scaled Gaussians, then the curvature inflection points are marked in the $s-\sigma$ plane. Finally they match the obtained curvature scale-space images instead of matching contours directly. They have refined [13] this representation by renormalization and by resampling the arc-length of curves to recognize them in case of nonuniform noise.

Asada and Brady [1] have proposed another technique, the *curvature primal sketch*, to depict a $2D$ curve in scale space. They first examine the behavior of a set of primitives (parameterized analytic curves) over a range of scales, then they produce a multiscale representation of the original parameterized contour by interpreting its significant changes in curvature as the instances of the primitives. However, this method depends on the choice of primitives, and the various types of primitives can be transformed into each other as scale changes.

A parsing algorithm, called *spatial stability analysis*, has been published by Bischoff and Caelli [3]. It allows the localization of region boundaries from scale-space image based on the observation that their zero-crossings remain spatially stable over changes in scale (which itself is a generalization of Witkin's stability criterion). The zero-crossings of the Laplacian are searched in a σ-proportional neighborhood, and their stability is measured via the maximum number of different scales at which the zero-crossings exist.

Gauch and Pizer [6] have presented two methods of identifying and analyzing the *multiresolution behavior* of ridges and valleys in $2D$ gray-scale images.

The first method uses the tools of differential geometry to associate the tops of intensity ridges and the bottoms of intensity valleys with corner points. The second technique is based on global drainage patterns of rainfall on a terrain map. The resulting watershed boundaries also identify the tops of ridges and the bottoms of valleys. Both representation s are studied as blurring proceeds, and by following their change, resolution hierarchies of ridges and valleys can be established.

Finally, we close this short overview by a reference to the *statistical analysis* in scale space performed by Topkar and Sood [19], where they have investigated how the strength of input noise affects scale space.

3 Creation of scale-space images

Let us examine some aspects of our first task: how to construct discretized scale-space images. The way to obtain a multiresolution image is simple in theory: we need only to smooth the initial image with the (derivatives of a) Gaussian of increasing variance σ. In practice, however, several problems arise because of the discretization.

The first is how to sample the continuous multiresolution image (i.e. at what values of σ) to get appropriate discrete versions. It is well-known in information theory that logarithmic sampling leads to informationally uniform sampling density. So the natural scale along the resolution axis is given by

$$\sigma_i = \varepsilon \cdot \tau^i$$

where the "hidden scale" ε takes care of the pixel size of the original image (see Romany et al [15, 14]). Namely, the initial image can only be considered as the lowest level of the discrete scale-space image if it has high quality. Even if it is true (but how can it be decided in advance ?), it is more straightforward to use the ε-smoothed image as the ground level. This way each level of the *multiresolution extension* image (smoothed by the Gaussian itself) corresponds to a level of the *scaled differential descriptors* (smoothed by the derivatives of the Gaussian); thus we simultaneously differentiate and scale the image.

The next problem relates to the filter: the Gaussian is continuous and has infinite support. Lindeberg et al [9, 5] proposed a discrete kernel to overcome

this problem; the suggested kernel approximates the Gaussian as its scale increases, but contrary to the Gaussian, it cannot be implemented at the same time in an isotropic and separable way. More efficient convolution techniques are based on the use of separable recursive filters, first introduced by Deriche, and extended also to the recursive implementation of the Gaussian and its derivatives [4]. Though the fact that the number of operations is independent of the kernel size is very attractive, we have found that non-linear combinations of derivatives may accumulate computational errors, possibly leading to inaccurate differential descriptors. Therefore, we prefer to use a separable sampled Gaussian with appropriate normalization, and to choose the kernel size so that only some δ percentage of its energy is lost. Computation of the kernel size $2a+1$ subject to relative δ error is very simple. Performing $2D$ integration we find:

$$\frac{1}{(2\pi)\sigma^2}\int\int_{-a}^{a} e^{-\frac{x^2+y^2}{2\sigma^2}}\,dxdy = 1 - e^{-\frac{a^2}{2\sigma^2}}$$

Since the integral of the Gaussian in the $x-y$ plane is 1, we immediately have the error part δ and the size a:

$$\begin{aligned}\delta &= e^{-\frac{a^2}{2\sigma^2}}\\ a &= \sqrt{-2\ln\delta}\cdot\sigma\end{aligned}$$

Similar expressions can also be derived for any derivative; a becomes larger as the derivative order increases, which is not surprising, since the derivatives tend to be more flattened. Normalization is done by multiplying the sampled filter coefficients so that their sum over the half kernel size $[-a\,..\,0]$ should be the theoretical value. Moreover, convolution with the filter should yield the correct derivatives when applied to simple polynomials.

Finally, we have to compute the scaled differentials correctly. For the continuous case there are, in principle, two equivalent ways to calculate them: by differentiating the smoothed signal or by convolving the signal with the differentiated smoothing kernel. This comes from the linearity of the Gaussian, which can be formulated as

$$L[f(\mathbf{r}) * g(\mathbf{r},\sigma)] = f(\mathbf{r}) * L[g(\mathbf{r},\sigma)]$$

where L is a linear differential operator and $*$ denotes convolution. However, in the discrete case, this is no longer true [9, 5]: a differential operator with small

support applied to an image blurred with an operator having large support shows the local changes of structure, but not the global ones as expected. Figure 4 illustrates this property with a synthetic image of an ellipse, where the extrema of the isophote curvature computed in two ways. In the first picture the augmenting support smoothing was followed by small support differential operators, and here only local patterns can be observed. However, in the second picture, which was generated by augmenting support differential operators, the four expected extrema can be seen.

To summarize, we have implemented an algorithm that convolves the initial image with the desired combinations of derivatives of a Gaussian kernel as the variance increases. Parameters specify the derivatives to be used and the three smoothing factors: the initial variance (ε), the number of samples at the resolution axis (n) and the ratio of the largest kernel size (corresponding to σ_n) and of the initial image size.

4 Visualization

We now come to the core of the paper: how to visualize the deep structure of a scale-space image. We create the $(n+1)D$ multiresolution extension of the nD original image and also the $(n+1)D$ image of a chosen nD differential descriptor at increasing scales. The $(n+1)D$ hyper-iso-surface of the multiresolution extension image can show the development of the nD iso-surface as resolution varies, while the $(n+1)D$ zero-crossings of the scaled differential descriptor image can demonstrate how the number and location of singularities change. Moreover, the intersection of the two hyper-iso-surfaces (one of intensities, the other of zero-crossings) illustrates the orbits of features. This is particularly impressive starting from a planar image. In the sequel, we restrict ourselves to $2D$ images.

4.1 Multiresolution extension

The multiresolution extension is a family of subsequently blurred images, where small structures gradually annihilate. As we keep track of the monotonous destruction of details from one level to another, we find that small grey-level changes are not necessarily visible. However, observing the transformation of

a chosen descriptor is more apparent, a simple example is regarding the development of an iso-intensity-contour.

We have already used the intuitive notion of iso-contours ($2D$) and also of iso-surface($3D$), but to define them precisely, the following arbitrary choice (or its opposite) must be made, as pointed out by Thirion and Gourdon in [18].

Definition 1 *The iso-surface is the interface between the regions of the image f: $f \geq I$ (the inside) and $f < I$ (the outside), where I is a constant.*

To extract iso-surfaces and also their intersections (e.g. iso-contours), they implemented a smart algorithm, called "marching lines", which insures both sub-voxel accuracy and nice topological properties like connectivity, closeness and no self-intersection. All the pictures of this paper, showing iso-surfaces, are obtained using the Marching Lines algorithm.

The iso-contours extracted from decreasing levels of resolution become more and more "regular", that is sharp curvatures are attenuated and the differences between intensity values are weakened, leading to a bowl-like convex shape. Note that the sequence of iso-contours extracted independently from the members of a family of blurred images is equivalent to the hyper-iso-contour (i.e. an iso-surface) obtained from the multiresolution extension; assuming, that the same intensity constant I is used. We use this fact: instead of extracting the sequence of iso-contours individually, we extract directly the corresponding iso-surface.

For an illustration, let us examine the deformation of the contour extracted from a planar binary image showing two connected balls, see figure 5. As resolution is reduced, the evolution of this contour is demonstrated by an iso-surface: the coordinates of points are marked in the (x, y) plane, while the resolution is measured via the z axis. The delocalization effect can be immediately investigated due to the natural (e.g. not parameterized) coordinate system. We also observe that the connectivity of the iso-contour is not preserved: in the course of blurring, it splits into two, then merges, then splits again.

4.2 Scaled differential descriptors

Instead of analyzing the multiresolution behavior of the iso-intensity-surface, it is more advantageous to examine invariants that allow comparisons between

neighboring points. Such examples are the gradient strength (in $2D$),

$$\|\Delta f(x,y)\| = \sqrt{f_x^2 + f_y^2}$$

which is basically an edge detector operator, or the Laplacian (in $2D$),

$$\nabla f(x,y) = f_{xx} + f_{yy}$$

whose zero-crossings are also applied to detect closed contours. In case of medical image processing, the concept of curvature (rate of change of the rotation angle with respect to the arc-length increment) plays an important role. The geometrical invariants such as the isophote curvature in $2D$

$$c(x,y) = \frac{2f_x f_y f_{xy} - f_x^2 f_{yy} - f_y^2 f_{xx}}{(f_x^2 + f_y^2)^{3/2}}$$

or the principal curvatures in $3D$ are widely used. Their extrema: the corner points in $2D$ and the ridge lines in $3D$ are already established as significant features (see e.g. [17]). Here we specify corner points as the loci where the derivative of the curvature in the direction of the iso-line tangent changes its sign (see figure 1); while ridge lines are their extension to $3D$, corresponding to the successive loci of the iso-surface whose principal curvature is locally extremal.

Definition 2 *Corner points satisfy the extremality criterion* $e(x,y) = \nabla\, c(x,y) \cdot \mathbf{t} = 0$, *where* $\mathbf{t} = (-f_y, f_x)$ *is the tangent to the iso-line and* $\nabla c(x,y) = (c_x, c_y)$ *is the gradient of the curvature* $c(x,y)$. *We call the implicit curve* $e(x,y) = 0$ *the curvature curve, whose* intersection *with the iso-line* $f(x,y) = I$ *are the points of extremal curvatures.*

In the same way that iso-intensity-contours extend naturally into hyper-iso-contours in scale space, so do the singularities of the primal image (such as curvature curves). This means that singularities at different scales can be observed with the help of the zero-intensity-surface extracted from the image of scaled differential descriptors.

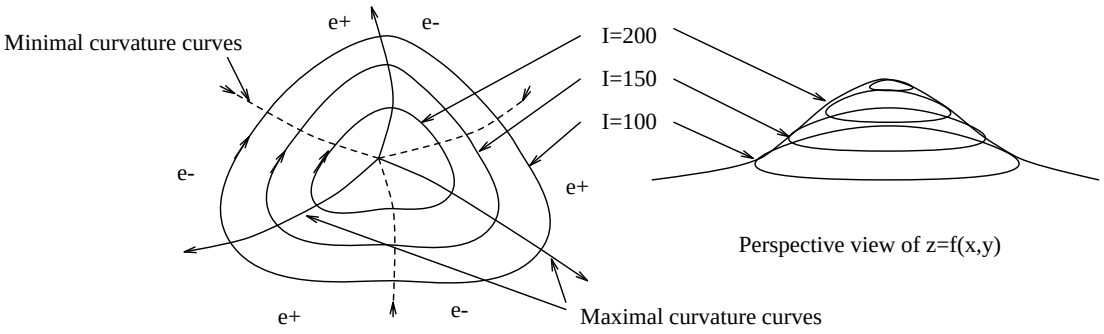

Figure 1: Corner points in $2D$

4.3 Integrating the information

We can display the sign of the scaled differentials, just like curvature extremality, on the iso-intensity-surface. More precisely, so as to deal with uncertainty, we can use three colors to separate definitely positive, definitely negative, and approximately zero valued regions. The uncertainty is for two reasons: Firstly, numerical errors can occur during computations because of floating point arithmetic. Secondly, even when the calculation is exact, the value of our descriptor may not change in an extended area, causing its derivatives to be zero. Hence it is not obvious where we should consider the change of sign; though we can use the same choice that was made at the definition of the iso-surface.

The figure 6 demonstrates this case. The sequence of iso-contours obtained from successively blurred ellipses is colored due to the sign of curvature extremality. There are two symmetrical zones corresponding to the smaller axis where the curvature is almost zero; here features are very unstable, their spatial positions and even their existences are not well defined.

Though coloring is an entirely reasonable form of visual description, we may need — to support further processing — a smaller and a more manageable representation of the information. We have already seen that corner points (ridge lines) are defined as the intersection of two iso-contours (surfaces). This indicates a natural way how the orbits of these features can be explicitly obtained in scale space: by intersecting two (hyper-)iso-contours: one

of the intensities, other of the zero-crossings. By following the orbits in scale space we can examine how bifurcations occur, that is, how a simple feature can turn into several features when the resolution is increased. Now we present an example starting from an MRI slice of the brain, see figures 7 and 8. The orbits of features (i.e. the loci where the scaled curvature extremality is zero) are marked by white lines, and we also display — as background information — the iso-surface extracted from the multiresolution extension which is colored according to the sign of the extremality.

However in practice, due to parser sampling along the resolution axis, it is hard to decide what orbit we should follow after a catastrophe point; figure 2 shows an example.

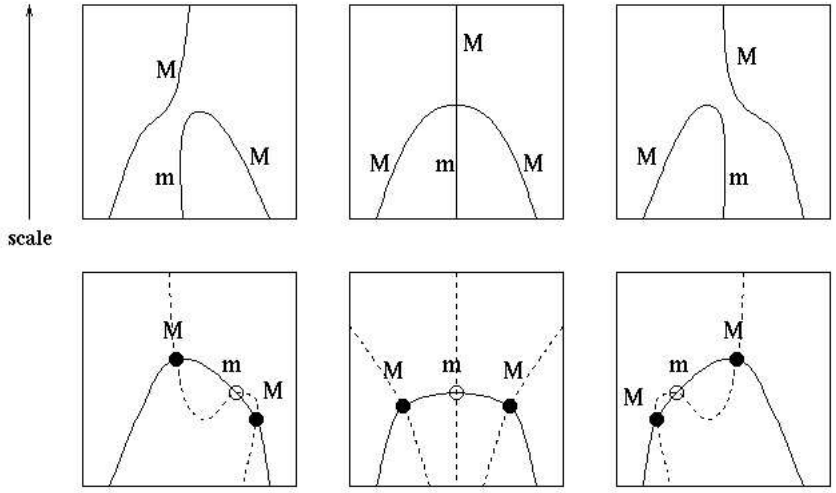

Figure 2: A small perturbation changes the symmetrical configuration (which is structurally unstable) *(down)* and as a consequence, the connection order of singularities in scale space *(top)*. Hence, at practically sparse sampling along the resolution axis, we have to deal with the uncertainty when following orbits from coarse to fine scale.

4.4 Scale is not equivalent to other dimensions

Finally, we discuss a natural question that may arise: why we *do not* extract directly the scaled features from the hyper-iso-contour, as we did extract directly the iso-intensity-surface of the multiresolution extension. To answer this question — for the clarity — let us restrict ourselves to the examination of corner points(the reasoning is very similar for higher dimensions and other invariants).

It seems natural, that instead of computing the sequence of corner pointsit is better to compute their $3D$ extensions, ridge lines. However, there is no sense to search for ridge lines on a hyper-iso-contour, because the two principal directions of the obtained surface generally do not correspond to the tangent of the iso-contours and to the (vertical) resolution axis. So the ridge lines do not correspond to the orbits of corner pointseither, that we can observe in figure 9 which shows the vector fields of the ellipse in figure 6.

5 Analyze of corner points in scale space

First, let us examine various types of characteristic curvature points: corner points (curvature extrema) and inflexion points (zero-crossings of curvature) with the help of table 1. The type of a point depends both on the magnitude and the sign of the curvature, while their significance is determined by the absolute value of the curvature. The absolute maxima of the curvature are generally more important features than the absolute minima, which can also be zero, i.e. points of inflexion. We cannot detect an inflexion point only with the extremality criterion; this is why we intend to study corner points as well as inflexion points.

The formula for curvature for iso-contours can be considered either as a $1D$ length-parameterized function or a $2D$ function of the variables x and y, where the latter form is obtained using the implicit function theorem [18]. It is interesting to compare curvature extrema to $1D$ intensity extrema (critical points) which have already been studied in scale space [21, 2, 22, 7]: the orbits of $1D$ intensity extrema are either lines from small to large scale or bowl-like shapes corresponding to a maximum point (**M**) and a minimum point (**m**) that merge at some catastrophe point.

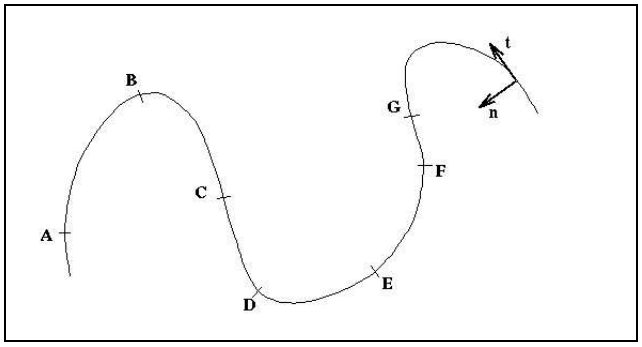

points	A	B	C	D	E	F	G
curvature	+	+	+ → -	-	-	-	- → +
extremality criterion	- → +	+ → -	- → -	- → +	+ → -	- → +	+ → +
type (value)	**m+**	**M+**	**infl.**	**m-**	**M-**	**m-**	**infl.**
significance (abs. value)	**m**	**M**	**m**	**M**	**m**	**M**	**m**

Table 1: Description of various types of characteristic curvature points (**m**: minimum, **M**: maximum)

The orbits of corner points, and also of inflexion points, have analogous structures, as it can be depicted in figure 10. Inflexion points may either survive or form a parabola as they merge at some scale, where the two branches of the parabola consist of points with - → + or + → - curvature change, respectively. Similarly, the structure of orbits in the case of corner points depends only on the transition of the extremality criterion, which means that the structure is independent of the sign of extrema (see table 1). This has the consequence that the significant and practically more stable absolute maxima (**M+** and **m-**) form such a sub-structure which makes their orbits difficult to follow. Indeed, because of the influence of a neighboring inflexion point, the sign of a curvature extremum may change as **M+** → **M-** and **m-** → **m+**, respectively (see figure 3). We call the intersection point of an extremum and an inflexion orbit *second order nongeneric singularity*, since at that point a second order

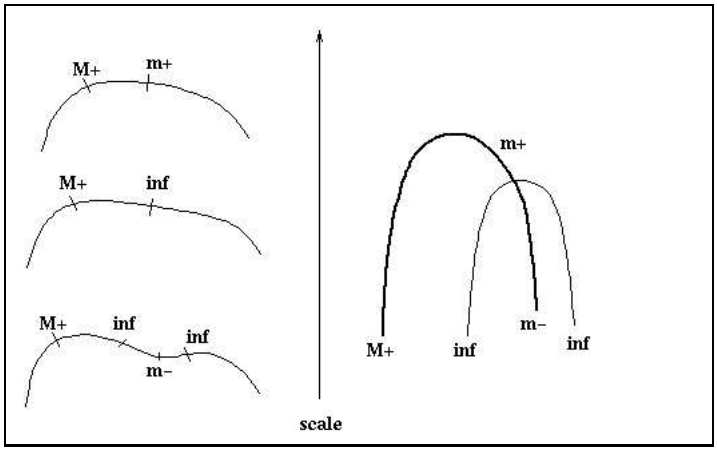

Figure 3: The sign of minimum *(thick line)* changes due to an inflexion point *(thin line)*

differential function, and also its gradient, a third order differential function, is zero.

We have found that an orbit which is relatively extended along the scale axis, but also has a small "base", indicates the presence of a highly curved feature of limited extent, i.e. a visually significant feature. Also, we can perceive that at some almost-straight contour-parts second order nongeneric singularities occur either at relatively fine scales or at large scales but with great "extent". These observations suggest that stability of corner points should be measured as the ratio of life-time delimited by second order nongeneric singularities and of base in scale space.

Definition 3 *The effective life-time T_e of a corner point is defined to be:*

- *the scale of intersection,*
  if its orbit is intersected by an inflexion orbit;
- *the scale of merging,*
  else if its orbit merges with another corner orbit
  (whereon both annihilates);
- *else, the largest scale of observation.*

Definition 4 *The base B of a corner point is defined to be:*

- *the Euclidean distance between the two branches of the inflexion parabola at the finest scale,*
  if its orbit is intersected by an inflexion orbit;
- *the Euclidean distance between the two branches of the obtained parabola at the finest scale,*
  else if its orbit merges with another corner orbit
  (whereon both annihilates);
- *else, one.*

Remark: it is worth measuring the distance as the Euclidean distance of the coordinates of points, and not as some path-length of the iso-contour (the latter one depends on the parameterization and we do not need it for the extraction).

6 Conclusion

We have presented a natural way to extract and represent multiscale singularity orbits based on iso-surface techniques. We have illustrated our ideas starting from planar (synthetic and real medical) images. We have shown that the representation is very convenient for observing both bifurcation and delocalization effects. It is also applicable to observe boundary evolution in scale space, assuming that the boundary can be defined as an iso-surface, for example the zero-crossings of the Laplacian of the intensity. In particular, we have analyzed the behavior of corner points and of curvature inflexion points in scale space. Based on our experiments we have proposed a stability criterion for corner points in terms of scale-space life-time and base. We believe that this method can help further understanding of the multiresolution properties of differential singularities.

Currently, the marching lines algorithm, which can extract iso-surfaces and their intersections (iso-lines), is implemented in $3D$, so it applies to the multiscale analysis of 2D images. In the future we intend to extend this algorithm to higher dimensions, to be able to investigate the multiresolution behavior of features of real $3D$ images.

Acknowledgment

We wish to thank Mike Brady and the members of the Epidaure research team for stimulating discussions about scale space. Part of this study has been supported by the Esprit Basic Research Action VIVA and the French-Hungarian Cooperation Program BALATON. Thanks also to Digital Equipment who provided us with fast computers.

References

[1] Haruo Asada and Michael Brady. The curvature primal sketch. *IEEE PAMI*, 8, 1986.

[2] Jean Babaud, P. Witkin, Andrew, Michael Baudin, and O. Duda, Richard. Uniqueness of the gaussian kernel for scale space filtering. *IEEE PAMI*, 8, Jan 1986.

[3] Walter F. Bischoff and Terry Caelli. Parsing scale-space and spatial stability analysis. *CVIGP*, 42(192-205), 1986.

[4] Rachid Deriche. Recursively implementing the gaussian and its derivatives. Technical report, INRIA, 1993.

[5] Jan-Olof Eklundh and Tony Lindeberg. On the computation of a scale-space primal sketch. 1990. Submitted to ECCU.

[6] John M. Gauch and Stephen M. Pizer. Multiresolution analysis of ridges and valleys in grey-scale images. *IEEE PAMI*, 15, 1993.

[7] Peter Johansen. On the classification of toppoints in scale space. *Journal of Mathematical Imaging and Vision*, 4:57–67, 1994.

[8] Jan J. Koenderink. The structure of images. *Biological Cybernetics*, 50:363–370, 1984.

[9] Tony Lindeberg. Scale-space for discrete signals. *IEEE PAMI*, 12, March 1990.

[10] Tony Lindeberg. Scale-space behaviour of local extrema and blobs. *Journal of Mathematical Imaging and Vision*, 1:65–99, March 1992.

[11] William E. Lorensen and Harvey E. Cline. Marching cubes: A high resolution 3d surface reconstruction algorithm. *Computer Graphics*, 21(4), July 1987.

[12] Farzin Mokhtarian and Mackworth Alain K. Scale-based description and recognition of planar curves and two-dimensional shapes. *IEEE PAMI*, 8, Jan 1986.

[13] Farzin Mokhtarian and Mackworth Alain K. A theory of multiscale, curvature-based representation for planar curves. *IEEE PAMI*, 14, Aug 1992.

[14] Bart M. ter Haar Romeny and Luc M. J. Florack. *Multiscale Geometric Model of Human Perception*, volume 511, chapter 4, pages 73–114. Springer-Verlag, 1993.

[15] Bart M. ter Haar Romeny, Luc M. J. Florack, Jan J. Koenderink, and Max A. Viergever. Scale space: Its natural operators and differential invariants. In *LNCS*, volume 511, pages 239–255. July 1991.

[16] D. Rotem and Y. Y. Zeevi. Image reconstruction from zero crossings. *IEEE ASSP*, 34:1269–1277, 1986.

[17] J-P. Thirion. The extremal mesh and the understanding of 3d surfaces. In *IEEE Workshop on Biomedical Imaging*, number 2149, Seattle, June 1994.

[18] J-P. Thirion and A. Gourdon. The 3d marching lines algorithm : new results and proofs. *Rapport de Recherche INRIA*, (1881), March 1993.

[19] V. A. Topkar and A. K. Sood. Statistical analysis of scale-space. *Signal Processing*, 26(307-334), 1992.

[20] Jayaram K. Udupa. Multidimensional digital boundaries. *CVGIP: Graphical Models and Image Processing*, 56, July 1994.

[21] P. Witkin, Andrew. Scale space filtering. In *Proc. Int. Conf. Artificial Intelligence*, volume 511, 1993. Karlsruhe.

[22] Alan L. Yuille and Tomaso A. Poggio. Fingerprint theorems for zero crossings. *Journal Opt. Soc. Amer.*, pages 683–692, 1985.

[23] Alan L. Yuille and Tomaso A. Poggio. Scaling theorems for zero crossings. *IEEE PAMI*, 8, 1986.

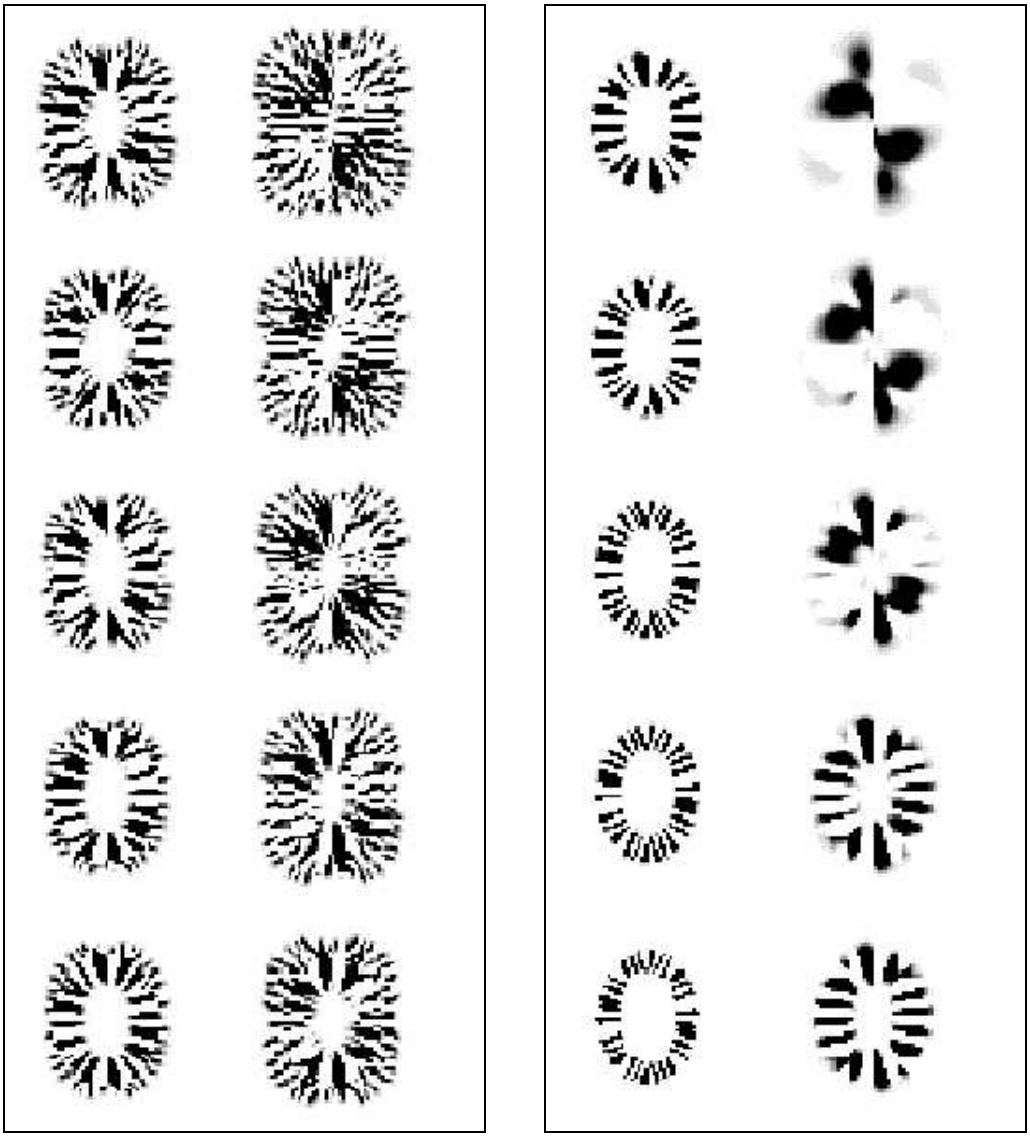

Figure 4: The extrema of the isophote curvature on an ellipsoidal function $i = ax^2 + by^2$ are computed in two ways. *left:* The augmenting support smoothing was followed by small support differential operators, and here only local patterns can be observed. *right:* However, in the case of augmenting support differential operators, the four expected extrema can be seen.

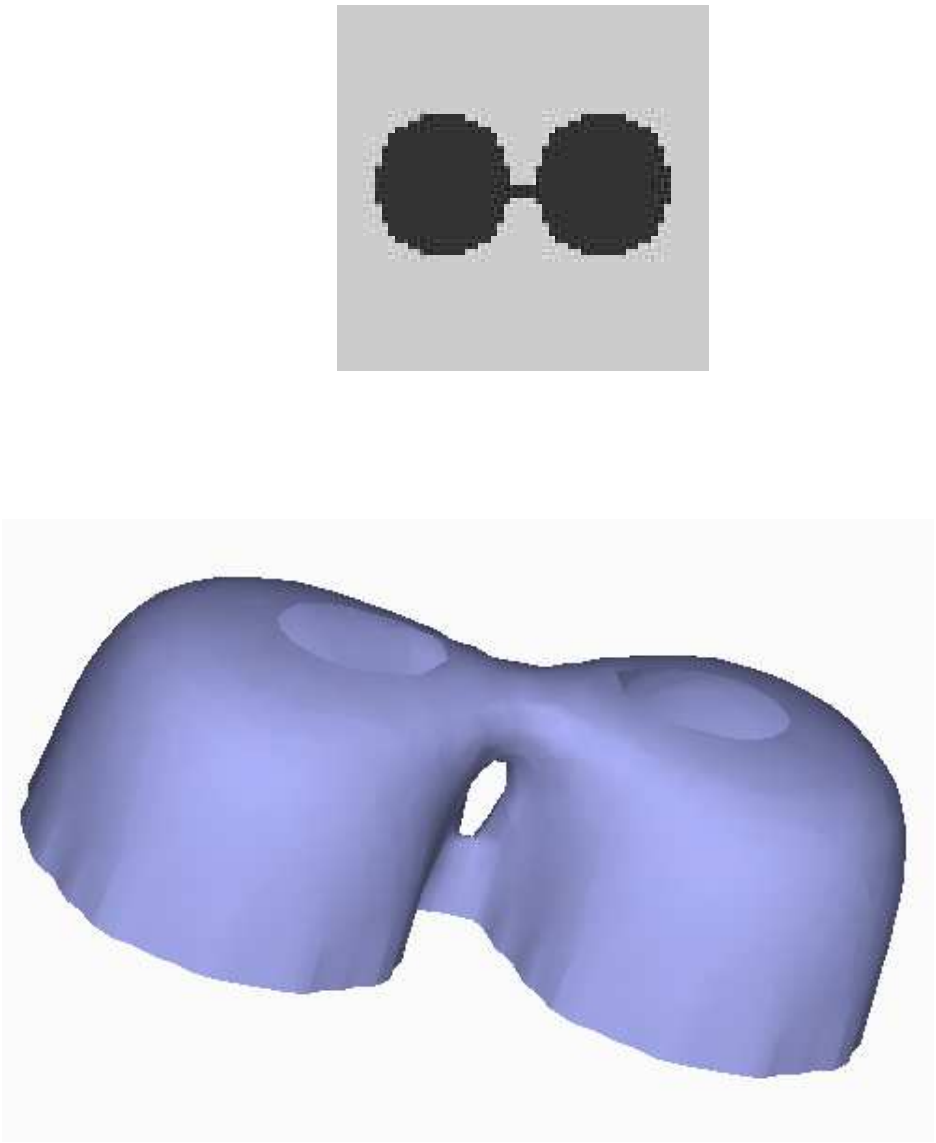

Figure 5: Original image *(above)* and its multiscale iso-contour *(below)* The coordinates of points are marked in the (x, y) plane, while resolution is measured via the z axis. The delocalization effect can be immediately investigated due to the natural (e.g. not parameterized) coordinate system. We also observe that the connectivity of the iso-contour is not preserved: in the course of blurring, it splits into two, then merges and then splits again.

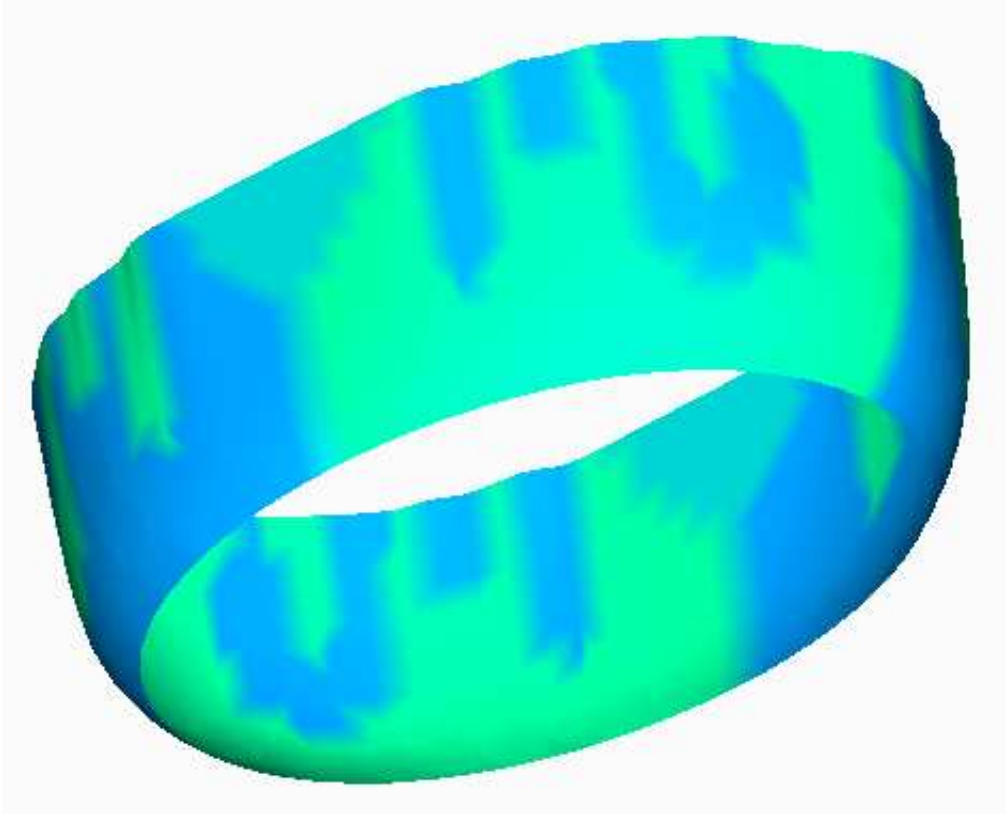

Figure 6: The scaled iso-contours of an ellipse are colored due to the sign of curvature extremality. There are two symmetrical zones corresponding to the smaller axis where the curvature is almost zero; here features are very unstable, their spatial positions and even their existences are not well defined.

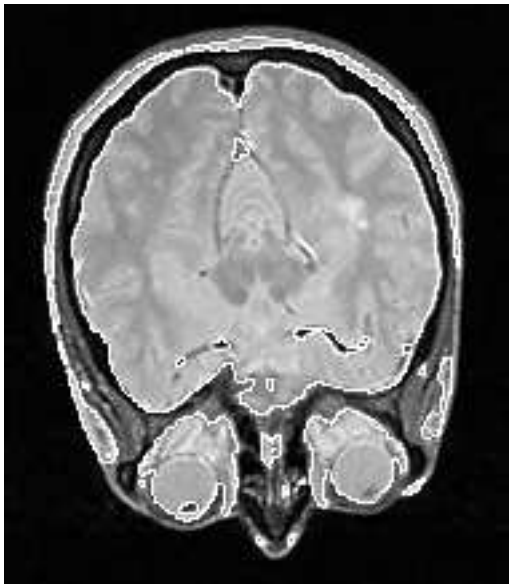

Figure 7: MRI slice of the brain with the selected iso-contour, the corresponding orbits of corner points are shown on the next page.

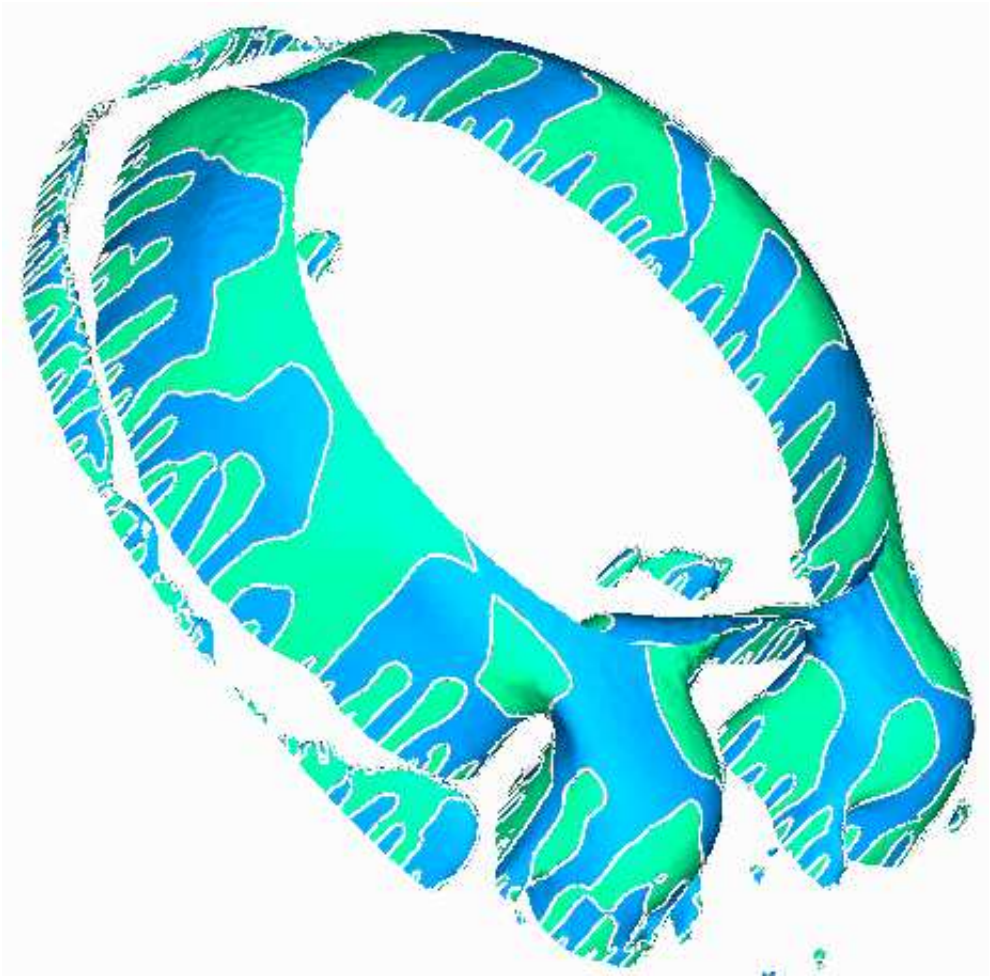

Figure 8: The orbits of corner points (i.e. the loci where the scaled curvature extremality is zero) are marked by white lines, and we also display — as background information — the multi-scale contour which is colored according to the sign of the extremality.

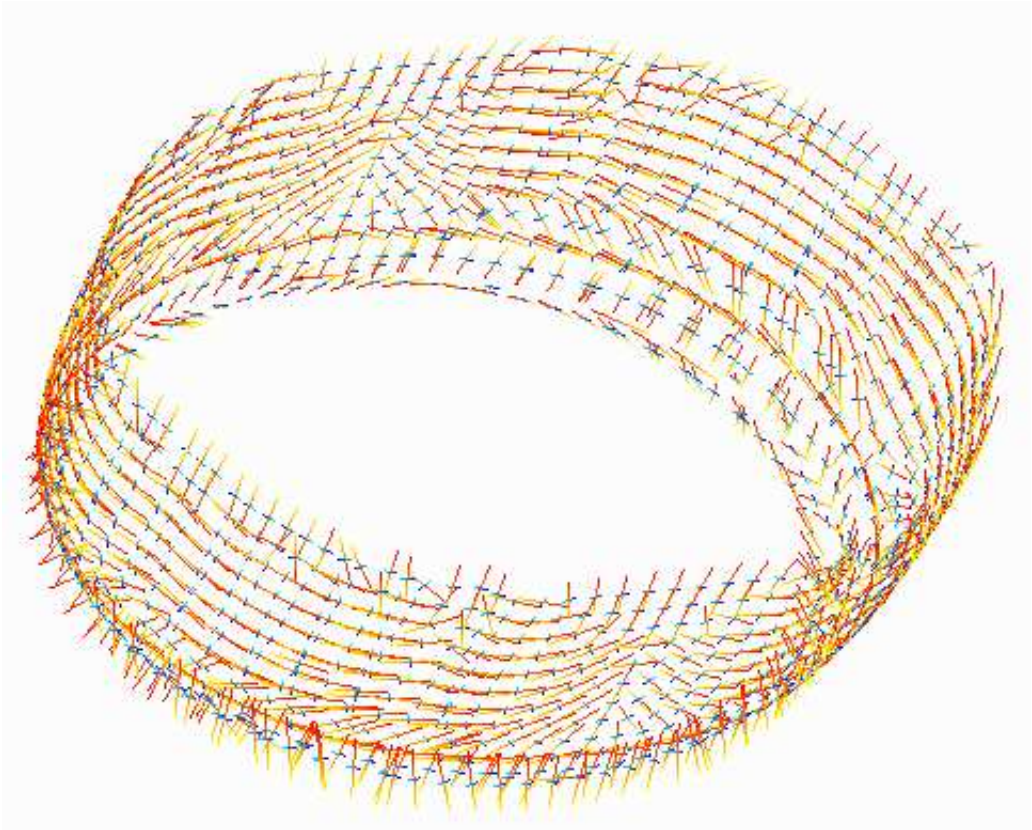

Figure 9: The principal direction fields of the same ellipsoid show that the orbits of corner points do not correspond to ridge lines. Since the two principal directions of the surface (i.e. multi-scale iso-contour) generally do not correspond to the tangent of the iso-contours and to the (vertical) resolution axis.

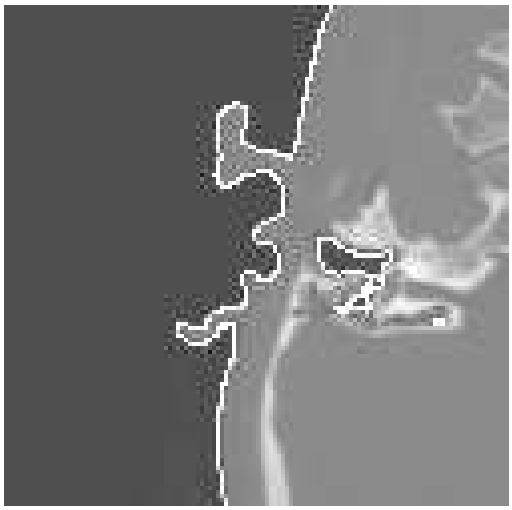

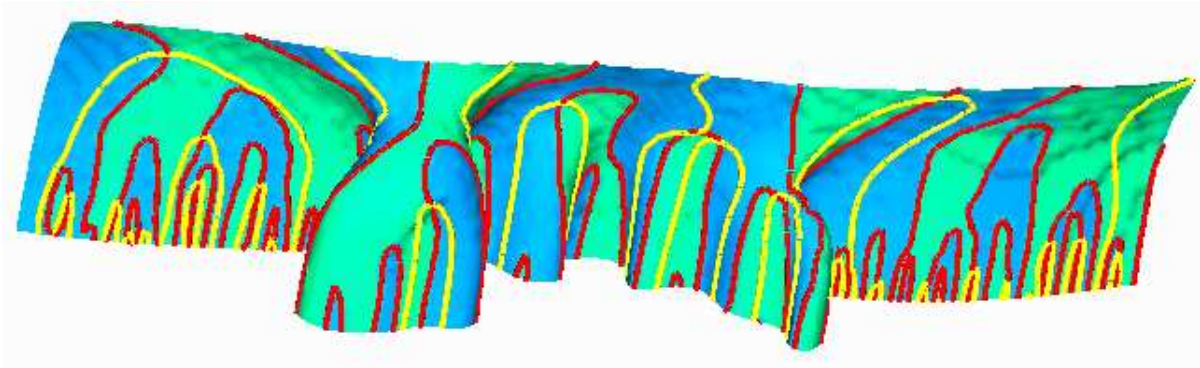

Figure 10: *above:* CT scan cross section of the ear with the selected iso-contour *below:* The orbits of inflexion (yellow) and of corner points (red) are marked on the multi-scale contour which is colored according to the sign of the curvature extremality.

Unité de recherche INRIA Lorraine, Technopôle de Nancy-Brabois, Campus scientifique,
615 rue du Jardin Botanique, BP 101, 54600 VILLERS LÈS NANCY
Unité de recherche INRIA Rennes, Irisa, Campus universitaire de Beaulieu, 35042 RENNES Cedex
Unité de recherche INRIA Rhône-Alpes, 46 avenue Félix Viallet, 38031 GRENOBLE Cedex 1
Unité de recherche INRIA Rocquencourt, Domaine de Voluceau, Rocquencourt, BP 105, 78153 LE CHESNAY Cedex
Unité de recherche INRIA Sophia-Antipolis, 2004 route des Lucioles, BP 93, 06902 SOPHIA-ANTIPOLIS Cedex

Éditeur
INRIA, Domaine de Voluceau, Rocquencourt, BP 105, 78153 LE CHESNAY Cedex (France)
ISSN 0249-6399